# Diffractive $\rho$ production at small x in future Electron - Ion Colliders

V. P. Gonçalves <sup>1,2</sup>, F. S. Navarra <sup>3</sup> and D. Spiering <sup>3</sup>
<sup>1</sup> Department of Astronomy and Theoretical Physics, Lund University, 223-62 Lund, Sweden.
<sup>2</sup> Instituto de Física e Matemática, Universidade Federal de Pelotas,
Caixa Postal 354, CEP 96010-900, Pelotas, RS, Brazil and
<sup>3</sup> Instituto de Física, Universidade de São Paulo, CEP 05315-970 São Paulo, SP, Brazil.

In this paper we complement previous studies of exclusive processes in future electron-ion (eA) colliders presenting a comprehensive analysis of diffractive  $\rho$  production at small x. We compute the coherent and incoherent cross sections using on the color dipole approach, taking into account non linear QCD dynamical effects and considering different models for the dipole - proton scattering amplitude and for the vector meson wave function. The dependencies of the cross sections with the energy, photon virtuality, nuclear mass number and squared momentum transfer are analysed in detail. Moreover, we compare the non linear predictions with those obtained in the linear regime. Finally, the predictions for  $\rho$  production are compared with those for other exclusive final states. Our results demonstrate that the analysis of diffractive  $\rho$  production in future electron - ion colliders will be important to understand the non linear QCD dynamics.

PACS numbers: 12.38.-t,13.60.Hb, 24.85.+p

#### I. INTRODUCTION

One of the main goals of the future Electron - Ion Colliders (EIC) [1-4] is the study of the hadronic structure in the non-linear regime of the Quantum Chromodynamics (QCD). Theoretically, we expect that the nuclei amplify the magnitude of the non-linear effects, which should allow to determine the presence of gluon saturation effects, its magnitude and what is the correct theoretical framework for their description (For reviews see, e.g., Ref. [5]). During the last years many authors have proposed the study of several inclusive and diffractive observables [6-22] in order to search for non linear effects in eA collisions. One of the most promising observables is exclusive production of vector mesons or photons, which are experimentally clean and can be unambiguously identified by the presence of a rapidity gap in final state. As these processes are driven by the gluon content of the target, with the cross sections being proportional to the square of the scattering amplitude, they are strongly sensitive to the underlying QCD dynamics. The diffractive production of  $J/\Psi$  and  $\phi$  in eA processes was analysed in detail in Refs. [14, 16–19] taking into account the non linear effects, and predictions for the energy, virtuality and transverse momentum dependencies were presented. In contrast, in the case of  $\rho$  production, only predictions for the energy and virtuality dependencies were presented in Refs. [14, 17]. Our goal in this paper is to complement and extend these previous studies and present a comprehensive analysis of  $\rho$  production. We present, for the first time, predictions for the distributions of the squared momentum transfer (t), which are an important source of information about the spatial distribution of the gluons in a nucleus and about fluctuations of the nuclear color fields, taking into account non linear QCD effects. We consider different models for the dipole - proton scattering amplitude as well as for the vector meson wave function. Moreover, we present a comparison between the non linear predictions with those obtained using a linear model for the QCD dynamics. Finally, we will compare the predictions for the  $\rho$  production with those for other exclusive final states.

This paper is organized as follows. In the next Section we present a brief review of the description of the diffractive  $\rho$  production in the color dipole formalism. In Section III we present our results for the energy, virtuality and momentum transfer dependencies of the  $\rho$  cross section. Finally, in Section IV we summarize our main conclusions.

#### II. DIFFRACTIVE $\rho$ PRODUCTION IN THE COLOR DIPOLE PICTURE

In the color dipole picture the diffractive  $\rho$  production in electron-nucleus interactions at high energies  $(eA \to e\rho Y)$  can be factorized in terms of the fluctuation of the virtual photon into a  $q\bar{q}$  color dipole, the dipole-nucleus scattering by a color singlet exchange and the recombination into the exclusive final state  $\rho$ , being characterized by a rapidity gap in the final state. The dipole - nucleus interactions can be classified as coherent or incoherent. If the nucleus scatters elastically, Y = A, the process is called coherent production and can be represented by the diagram in Fig. 1 (left panel). On the other hand, if the nucleus scatters inelastically, i.e. breaks up (Y = A'), the process is denoted incoherent production and can be represented as in Fig. 1 (right panel).

In the coherent case, the corresponding integrated cross section can be expressed in the large coherence length limit

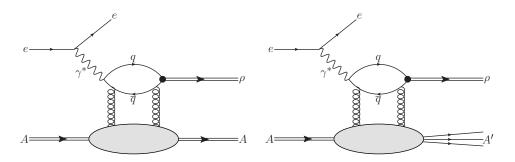


FIG. 1: Diffractive  $\rho$  production in coherent (left panel) and incoherent (right panel) eA collisions.

 $(l_c \gg R_A)$  as [14, 23]

$$\sigma^{coh}\left(\gamma^*A \to \rho A\right) = \int d^2 \boldsymbol{b} \left\langle \mathcal{N}^A(x, \boldsymbol{r}, \boldsymbol{b}) \right\rangle^2 \tag{1}$$

where

$$\langle \mathcal{N}^A \rangle = \int d^2 \mathbf{r} \int dz \, \Psi_{\rho}^*(\mathbf{r}, z) \, \mathcal{N}^A(x, \mathbf{r}, \mathbf{b}) \, \Psi_{\gamma^*}(\mathbf{r}, z, Q^2) \; . \tag{2}$$

In the above expression  $\Psi_{\gamma^*}(\boldsymbol{r},z,Q^2)$  and  $\Psi_{\rho}(\boldsymbol{r},z)$  are the wave functions of the virtual photon and  $\rho$  meson respectively, with  $\boldsymbol{r}$  and z being the dipole transverse radius and the momentum fraction of the photon carried by a quark (an antiquark carries then 1-z). Also, in the above formulas  $\mathcal{N}^A(x,\boldsymbol{r},\boldsymbol{b})$  is the forward dipole-nucleus scattering amplitude (for a dipole at impact parameter  $\boldsymbol{b}$ ) which encodes all the information about the hadronic scattering, and thus about the non linear and quantum effects in the hadron wave function. The amplitude  $\mathcal{N}^A$  depends on the  $\gamma$  – hadron center - of - mass reaction energy, W, through the variable:

$$x = \frac{Q^2 + m_V^2}{Q^2 + W^2} \tag{3}$$

where  $Q^2$  and  $m_V$  are the photon virtuality and vector meson mass, respectively. From this definition it is clear that when  $Q^2 = 0$  the cross section for  $\rho$  production is much more sensitive to low x effects than the one for production of heavy mesons. The differential distribution with respect to the squared momentum transfer t for coherent interactions is given by

$$\frac{d\sigma_{coh}}{dt} = \frac{1}{16\pi} \left| \mathcal{A}^{\gamma^* A \to \gamma A}(x, Q^2, t) \right|^2,\tag{4}$$

where

$$\mathcal{A}^{\gamma^* A \to \gamma A}(x, Q^2, t) = 2 \int d^2 \boldsymbol{b} \, e^{-i\boldsymbol{b} \cdot \Delta} \langle \mathcal{N}^A(x, \boldsymbol{r}, \boldsymbol{b}) \rangle, \tag{5}$$

with  $\Delta^2 = -t$ .

For incoherent interactions, one sums over all final states of the target nucleus, except those that contain particle production. Therefore we have:

$$\sigma^{inc}\left(\gamma^* A \to \gamma A'\right) = \frac{|\mathcal{I}m \,\mathcal{A}(s, t=0)|^2}{16\pi \,B} \tag{6}$$

where at high energies  $(l_c \gg R_A)$  [23]:

$$|\mathcal{I}m\,\mathcal{A}|^2 = \int d^2\boldsymbol{b}\,A\,T_A(\boldsymbol{b}) \left\langle \sigma_{dp}\,\exp\left[-\frac{1}{2}\,\sigma_{dp}\,A\,T_A(\boldsymbol{b})\right]\right\rangle^2 \tag{7}$$

with the t slope (B) being the same as in the case of a nucleon target. In the incoherent case, the  $q\bar{q}$  pair attenuates with a constant absorption cross section, as in the Glauber model, except that the whole exponential is averaged rather than just the cross section in the exponent. For the calculation of the differential cross section  $d\sigma/dt$  for

Model	$M_{\rho}/{\rm GeV}$	$m_f/{\rm GeV}$	$N_T$	$R_T^2/{\rm GeV}^{-2}$	$R^2/{\rm GeV}^{-2}$	$N_L$	$R_L^2/{\rm GeV}^{-2}$
Gauss-LC	0.776	0.14	4.47	21.9	-	1.79	10.4
Boosted Gaussian	0.776	0.14	0.911	_	12.9	0.853	_

TABLE I: Parameters of the Gauss-LC and Boosted Gaussian models for the  $\rho$  wave function.

incoherent interactions we apply for the  $\rho$  production the treatment presented in Ref. [18]. Consequently, we have that

$$\frac{d\sigma_{inc}}{dt} = \frac{1}{16\pi} \left\langle \left\langle \left| \mathcal{A}^{\gamma^* A \to \gamma A'}(x, Q^2, t) \right|^2 \right\rangle \right\rangle, \tag{8}$$

with the scattering amplitude  $\mathcal{A}^{\gamma^*A\to\gamma A'}$  being approximated by [18]

$$|\mathcal{A}^{\gamma^* A \to \gamma A'}(x, Q^2, t)|^2 = 16\pi^2 B_p^2 \int d^2 \boldsymbol{b} e^{-B_p \Delta^2} \mathcal{N}^p(x, \boldsymbol{r}) \mathcal{N}^p(x, \boldsymbol{r}') A T_A(\boldsymbol{b})$$

$$\times \exp \left\{ -2\pi (A - 1) B_p T_A(\boldsymbol{b}) \left[ \mathcal{N}^p(x, \boldsymbol{r}) + \mathcal{N}^p(x, \boldsymbol{r}') \right] \right\}, \tag{9}$$

where  $B_p$  is associated to the impact parameter profile function in the proton and  $\mathcal{N}^p(x, \mathbf{r})$  is the dipole - proton scattering amplitude.

In order to estimate the coherent and incoherent cross sections we need to specify the wave functions and the dipole - nucleus  $\mathcal{N}^A(x, r, b)$  and dipole - proton  $\mathcal{N}^p(x, r)$  scattering amplitudes. Initially let us discuss the models used for the wave functions. In contrast to the photon wave function, which is well known in the literature (See e.g. [26]), the  $\rho$  wave function is still an open question. The simplest approach is to assume that the vector meson is predominantly a quark-antiquark state and that the spin and polarization structure is the same as in the photon [27–30] (for other approaches see, for example, Ref. [31]). As a consequence, the overlap between the photon and the vector meson wave function, for the transversely and longitudinally polarized cases, is given by (For details see Ref. [26])

$$(\Psi_V^* \Psi)_T = \frac{\hat{e}_f e}{4\pi} \frac{N_c}{\pi z (1-z)} \left\{ m_f^2 K_0(\epsilon r) \phi_T(r, z) - \left[ z^2 + (1-z)^2 \right] \epsilon K_1(\epsilon r) \partial_r \phi_T(r, z) \right\}, \tag{10}$$

$$(\Psi_V^* \Psi)_L = \frac{\hat{e}_f e}{4\pi} \frac{N_c}{\pi} 2Qz(1-z) K_0(\epsilon r) \left[ M_V \phi_L(r,z) + \delta \frac{m_f^2 - \nabla_r^2}{M_V z(1-z)} \phi_L(r,z) \right], \tag{11}$$

where  $\hat{e}_f$  is the effective charge of the vector meson,  $m_f$  is the quark mass,  $N_c = 3$ ,  $\epsilon^2 = z(1-z)Q^2 + m_f^2$  and  $\phi_i(r,z)$  define the scalar part of the vector meson wave functions. In what follows we will consider the Boosted Gaussian and Gauss-LC models for  $\phi_T(r,z)$  and  $\phi_L(r,z)$ , which are largely used in the literature. In the Boosted Gaussian model the function  $\phi_i(r,z)$  are given by

$$\phi_{T,L}(r,z) = N_{T,L} z(1-z) \exp\left[-\frac{m_f^2 R^2}{8z(1-z)} - \frac{2z(1-z)r^2}{R^2} + \frac{m_f^2 R^2}{2}\right].$$
(12)

In contrast, in the Gauss-LC model, it are given by

$$\phi_T(r,z) = N_T [z(1-z)]^2 \exp(-r^2/2R_T^2), \qquad (13)$$

$$\phi_L(r,z) = N_L z(1-z) \exp\left(-r^2/2R_L^2\right). \tag{14}$$

The parameters  $N_i$ , R and  $R_i$  are determined by the normalization condition of the wave function and by the decay width. In Table I we present the value of these parameters for the  $\rho$  wave function. It is important to emphasize that predictions based in these models for the wave functions have been tested with success in ep and ultra peripheral heavy ion collisions (See, e. g. Refs. [32, 33]).

Finally, let us discuss the models used in our calculations for  $\mathcal{N}^A(x, r, b)$  and  $\mathcal{N}^p(x, r)$ . As in our previous studies [14, 17, 22], in what follows we will use in our calculations the model proposed in Ref. [24], which describes the current experimental data on the nuclear structure function as well as includes the impact parameter dependence in the dipole nucleus cross section (For details see Ref. [13]). In this model the forward dipole-nucleus amplitude is given by

$$\mathcal{N}^{A}(x, \boldsymbol{r}, \boldsymbol{b}) = 1 - \exp\left[-\frac{1}{2}\sigma_{dp}(x, \boldsymbol{r}^{2}) A T_{A}(\boldsymbol{b})\right], \qquad (15)$$

where  $\sigma_{dp}$  is the dipole-proton cross section and  $T_A(\mathbf{b})$  is the nuclear profile function, which is obtained from a 3-parameter Fermi distribution for the nuclear density normalized to 1. This equation, based on the Glauber-Gribov formalism [25], sums up all the multiple elastic rescattering diagrams of the  $q\bar{q}$  pair and is justified for large coherence length, where the transverse separation  $\mathbf{r}$  of partons in the multiparton Fock state of the photon becomes a conserved quantity, *i.e.* the size of the pair  $\mathbf{r}$  becomes eigenvalue of the scattering matrix. Furthermore, the dipole-proton cross section  $\sigma_{dp}$  is given in the eikonal approximation by:

$$\sigma_{dp}(x, \mathbf{r}) = 2 \int d^2 \mathbf{b} \, \mathcal{N}^p(x, \mathbf{r}, \mathbf{b}) , \qquad (16)$$

where  $\mathcal{N}^p(x, r, b)$  is the imaginary part of the forward amplitude for the scattering between a small dipole (a colorless quark-antiquark pair) and a dense hadron target, at a given rapidity interval  $Y = \ln(1/x)$ . The dipole has transverse size given by the vector  $\mathbf{r} = \mathbf{x} - \mathbf{y}$ , where  $\mathbf{x}$  and  $\mathbf{y}$  are the transverse vectors for the quark and antiquark, respectively, and impact parameter  $\mathbf{b} = (\mathbf{x} + \mathbf{y})/2$ . At high energies the evolution with the rapidity Y of  $\mathcal{N}^p(x, \mathbf{r}, \mathbf{b})$  is given in the Color Glass Condensate (CGC) formalism [34] by the infinite hierarchy of equations, the so called Balitsky-JIMWLK equations [34, 35], which reduces in the mean field approximation to the Balitsky-Kovchegov (BK) equation [35, 36]. In what follows we will consider the numerical solution of the running coupling BK equation obtained in Ref. [37] (denoted rcBK hereafter) obtained assuming the translational invariance approximation, which implies  $\mathcal{N}^p(x, \mathbf{r}, \mathbf{b}) = \mathcal{N}^p(x, \mathbf{r})S(\mathbf{b})$  and  $\sigma_{dp}(x, \mathbf{r}) = \sigma_0 \cdot \mathcal{N}^p(x, \mathbf{r})$ , with the normalization of the dipole cross section ( $\sigma_0$ ) being fitted to data. It is important to emphasize that the normalization  $\sigma_0$  defines  $B_p$  in Eq. (9), since they are related:  $B_p = \sigma_0/4\pi$ . From what was said above, we can see that  $\mathcal{N}^p(x, \mathbf{r})$  is the main input for the calculation of the incoherent  $\rho$  cross section [See Eq. (9)]. For the sake of completeness, as in Ref. [22], we will also consider the phenomenological model proposed in Ref. [26] and recently updated in Ref. [38]. This model, denoted bCGC hereafter, is based on the CGC formalism and takes into account the impact parameter dependence of the dipole proton scattering amplitude. In the bCGC model the dipole - proton scattering amplitude is given by [26]

$$\mathcal{N}^{p}(x, \boldsymbol{r}, \boldsymbol{b}) = \begin{cases} \mathcal{N}_{0} \left( \frac{r Q_{s}(b)}{2} \right)^{2 \left( \gamma_{s} + \frac{\ln(2/r Q_{s}(b))}{\kappa \lambda Y} \right)} & r Q_{s}(b) \leq 2\\ 1 - e^{-A \ln^{2} \left( B \, r Q_{s}(b) \right)} & r Q_{s}(b) > 2 \end{cases}$$

$$(17)$$

with  $\kappa = \chi''(\gamma_s)/\chi'(\gamma_s)$ , where  $\chi$  is the LO BFKL characteristic function. The coefficients A and B are determined uniquely from the condition that  $\mathcal{N}^p(x, \boldsymbol{r}, \boldsymbol{b})$ , and its derivative with respect to  $rQ_s(b)$ , are continuous at  $rQ_s(b) = 2$ . In this model, the proton saturation scale  $Q_s(b)$  depends on the impact parameter:

$$Q_s(b) \equiv Q_s(x,b) = \left(\frac{x_0}{x}\right)^{\frac{\lambda}{2}} \left[\exp\left(-\frac{b^2}{2B_{\text{CGC}}}\right)\right]^{\frac{1}{2\gamma_s}}.$$
 (18)

The parameter  $B_{\text{CGC}}$  was adjusted to give a good description of the t-dependence of exclusive  $J/\psi$  photoproduction. Moreover, the factors  $\mathcal{N}_0$  and  $\gamma_s$  were taken to be free. The set of parameters which will be used here are the following:  $\gamma_s = 0.6599$ ,  $\kappa = 9.9$ ,  $B_{CGC} = 5.5 \text{ GeV}^{-2}$ ,  $\mathcal{N}_0 = 0.3358$ ,  $x_0 = 0.00105$  and  $\lambda = 0.2063$ .

#### III. RESULTS

We initially address the energy W and virtuality  $Q^2$  dependence of the coherent and incoherent cross sections considering two different nuclei: A = 40 (Ca) and 208 (Pb). In what follows, we shall use the Gauss-LC model for the overlap function. As expected, in Fig. 2 we observe that the cross sections increase with the energy and nuclear mass number and decrease with the photon virtuality. At large nuclei and small  $Q^2$  the predictions considering the rcBK and bCGC models as input are almost identical. On the other hand, at smaller nuclei and large  $Q^2$  these predictions start to differ and this can be traced back to the different behaviour predicted by these models for the transition between the linear and non linear regimes (See, e.g. Fig. 3 in Ref. [22]).

One of the reasons to study  $\rho$  production is that, as shown by HERA data, this process probes the transition between the soft and hard QCD regimes, with the energy dependence being strongly sensitive to  $Q^2$ . In order to check how this behaviour is modified by the nuclear medium, in Fig. 3 we present our predictions for the energy dependence of the coherent and incoherent cross sections, normalized to the unity at W=50 GeV. As in the proton case, the slope increases with the virtuality, with the growth being smaller for heavier nuclei. Moreover, we can observe that the energy dependence is strongly modified at larger nuclei and smaller  $Q^2$ . This behaviour is expected, since in this kinematical range the magnitude of the non linear effects is predicted to be amplified. At large  $Q^2$ , the difference between the slopes for different atomic mass number decreases, which is associated to the fact that the linear regime becomes dominant.

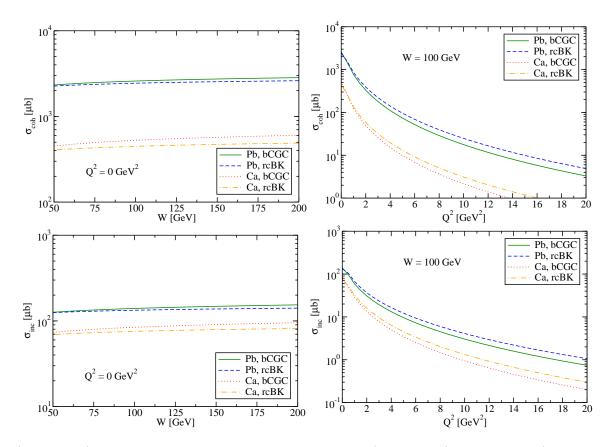


FIG. 2: (Color online) Energy and virtuality dependence of the coherent (upper panels) and incoherent (lower panels) cross sections for two different nuclei.

Let us now extend our analysis to the differential distributions  $d\sigma/dt$  for coherent and incoherent interactions. In Fig. 4 we present our predictions for the coherent and incoherent  $\rho$  cross section for different nuclei and  $Q^2 = 0$ . In particular, in the left panels we present our predictions considering different models for the dipole - proton scattering amplitude and in the right panels for different wave functions. We obtain that the coherent cross section clearly exhibits the typical diffractive pattern, with the dips in the range  $|t| \leq 0.3 \text{ GeV}^2$  increasing with the mass atomic number. Moreover, the positions of the dips are almost independent of the dipole - proton model used as input in the calculations, as already observed in Ref. [22] for the nuclear DVCS. Moreover, we obtain that our results are almost independent of the model used to calculate the wave functions. This conclusion is also valid for the incoherent cross section, which is slightly dependent on the model used for  $\mathcal{N}^p(x, r)$  for lighter nuclei. In Fig. 5 we present our predictions considering different values of  $Q^2$  and distinct nuclei. As expected, the cross sections decreases with the photon virtuality, with the position of the dips in the coherent cross sections being almost independent of  $Q^2$ .

Let us now compare our predictions for the  $\rho$  production with those for other exclusive final states:  $J/\Psi$ ,  $\phi$  and  $\gamma$ . In Fig. 6 we present our results for two different values of  $Q^2$  and A=Pb. For  $Q^2=0$  (upper panels) we have that the differential cross sections decrease at heavier vector mesons and the position of the dips for the  $J/\Psi$  production is slightly different of the other mesons, which is associated to the dominance of small dipoles in this final state. In contrast,  $Q^2=10~{\rm GeV^2}$  (lower panels), the position of the dips becomes almost identical for all exclusive final states.

Finally, in order to estimate the magnitude of the non linear effects, we present in Fig. 7 a comparison between our predictions and those obtained disregarding the multiple scatterings of the dipole with the nuclei and the presence of the non linear effects in the nucleon. Basically, we will assume as input in our calculations the following models for the scattering amplitudes:

$$\mathcal{N}^A(x,r,b) = \frac{1}{2}\sigma_{dip}(x,r)AT_A(b) \tag{19}$$

with  $\sigma_{dip}$  given by Eq. (16) and  $\mathcal{N}^p(x, \boldsymbol{r}, \boldsymbol{b})$  given by the linear part of the bCGC model

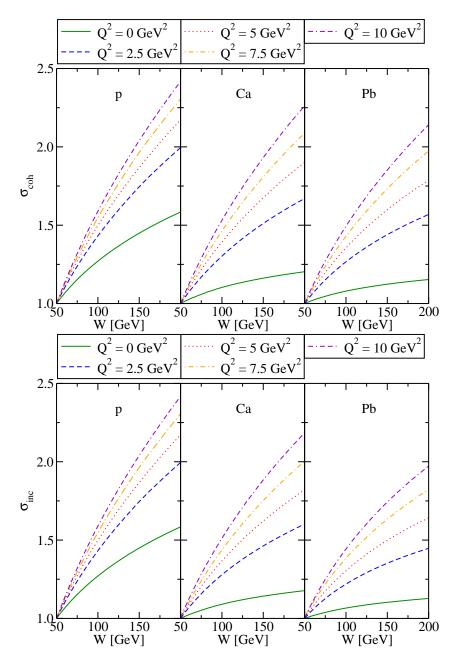


FIG. 3: (Color online) Energy dependence of the normalized coherent (upper panels) and incoherent (lower panels) cross sections for different photon virtualities  $Q^2$ . The predictions for the  $\rho$  production in ep collisions are presented for comparison.

$$\mathcal{N}^{p}(x, \boldsymbol{r}, \boldsymbol{b}) = \mathcal{N}_{0} \left( \frac{r Q_{s}(b)}{2} \right)^{2\left(\gamma_{s} + \frac{\ln(2/rQ_{s}(b))}{\kappa \lambda Y}\right)} . \tag{20}$$

We can observe that the incoherent cross sections are not strongly modified by the non linear effects. In contrast, in the case of coherent interactions, the magnitude of the cross section and position of the dips are distinct in the non linear and linear predictions, which makes the analysis of this observable a sensitive probe of the non linear QCD dynamics.

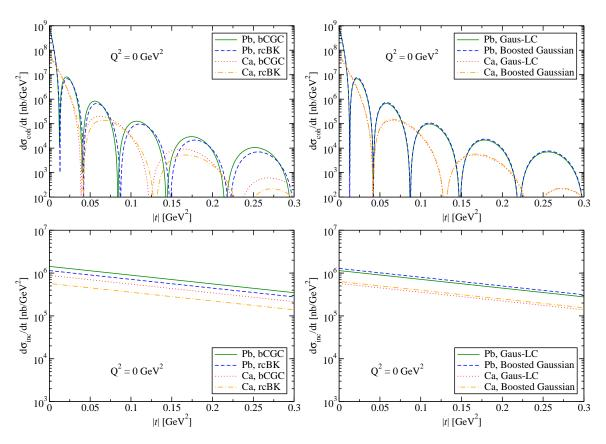


FIG. 4: (Color online) Differential cross section for coherent (upper panels) and incoherent (lower panels) interactions considering different models for the dipole - proton scattering amplitude (left panels) and distinct wave functions (right panels).

### IV. CONCLUSIONS

The study of exclusive processes in deep inelastic scattering (DIS) processes have been one of the main focuses of hadronic physics in the last years. It is expected that analysis of these processes allow us to probe the QCD dynamics at high energies, driven by the gluon content of the target (proton or nucleus) which is strongly subject to non linear effects (parton saturation) effects. In particular, electron - nucleus collisions the gluon density probed is amplified due to the coherent contributions from many nucleons. Our goal in this paper was extend and complement previous studies about the vector meson production in eA collisions, presenting a comprehensive analysis of the energy, virtuality, atomic mass number and transverse momentum dependencies of the cross section for the  $\rho$  production in the kinematical range which could be in future electron - ion colliders. We have obtained that the energy dependence of the differential cross sections are strongly modified with the increasing of the atomic mass number and that coherent cross section dominates at small t and the incoherent one at large t. Our results demonstrated that the number of dips at small t increases with the atomic number, with the position of the dips being almost independent of the model used to treat the dipole - proton interaction. Moreover, we shown that our predictions are insensitive to the model used to treat the  $\rho$  wave function. A comparison with other exclusive final states was presented and we have demonstrated that the non linear effects implies different positions for the dips in comparison to the linear one. These results are robust predictions from the saturation physics, which can be used to challenge the treatment of the non linear QCD dynamics in the kinematical range of future electron - ion experiments.

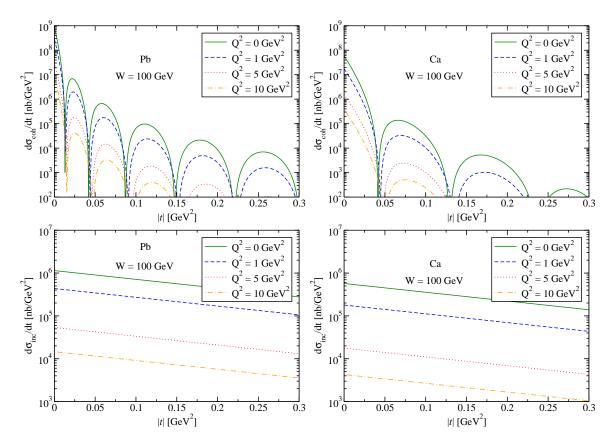


FIG. 5: (Color online) Differential cross section for coherent (upper panels) and incoherent (lower panels) interactions considering different values of  $Q^2$  and distinct nuclei.

## Acknowledgments

This work was partially financed by the Brazilian funding agencies CNPq, CAPES and FAPERGS.

<sup>[1]</sup> A. Deshpande, R. Milner, R. Venugopalan and W. Vogelsang, Ann. Rev. Nucl. Part. Sci. 55, 165 (2005).

<sup>[2]</sup> D. Boer, M. Diehl, R. Milner, R. Venugopalan, W. Vogelsang, D. Kaplan, H. Montgomery and S. Vigdor et al., arXiv:1108.1713 [nucl-th].

<sup>[3]</sup> A. Accardi, J. L. Albacete, M. Anselmino, N. Armesto, E. C. Aschenauer, A. Bacchetta, D. Boer and W. Brooks *et al.*, arXiv:1212.1701 [nucl-ex].

<sup>[4]</sup> J. L. Abelleira Fernandez et al. [LHeC Study Group Collaboration], J. Phys. G 39, 075001 (2012)

<sup>[5]</sup> F. Gelis, E. Iancu, J. Jalilian-Marian and R. Venugopalan, Ann. Rev. Nucl. Part. Sci. 60, 463 (2010); E. Iancu and R. Venugopalan, arXiv:hep-ph/0303204; H. Weigert, Prog. Part. Nucl. Phys. 55, 461 (2005); J. Jalilian-Marian and Y. V. Kovchegov, Prog. Part. Nucl. Phys. 56, 104 (2006); J. L. Albacete and C. Marquet, Prog. Part. Nucl. Phys. 76, 1 (2014).

<sup>[6]</sup> V. P. Goncalves, Phys. Lett. B 495, 303 (2000)

<sup>[7]</sup> M. S. Kugeratski, V. P. Goncalves and F. S. Navarra, Eur. Phys. J. C 46, 465 (2006)

<sup>[8]</sup> M. S. Kugeratski, V. P. Goncalves and F. S. Navarra, Eur. Phys. J. C 46, 413 (2006)

<sup>[9]</sup> N. N. Nikolaev, W. Schafer, B. G. Zakharov and V. R. Zoller, JETP Lett. 84, 537 (2007)

<sup>[10]</sup> H. Kowalski, T. Lappi and R. Venugopalan, Phys. Rev. Lett. 100, 022303 (2008)

<sup>[11]</sup> H. Kowalski, T. Lappi, C. Marquet and R. Venugopalan, Phys. Rev. C 78, 045201 (2008)

<sup>[12]</sup> E. R. Cazaroto, F. Carvalho, V. P. Goncalves and F. S. Navarra, Phys. Lett. B 669, 331 (2008)

<sup>[13]</sup> E. R. Cazaroto, F. Carvalho, V. P. Goncalves and F. S. Navarra, Phys. Lett. B 671, 233 (2009)

<sup>[14]</sup> V. P. Goncalves, M. S. Kugeratski, M. V. T. Machado and F. S. Navarra, Phys. Rev. C 80, 025202 (2009).

<sup>[15]</sup> V. P. Goncalves, M. S. Kugeratski and F. S. Navarra, Phys. Rev. C 81, 065209 (2010)

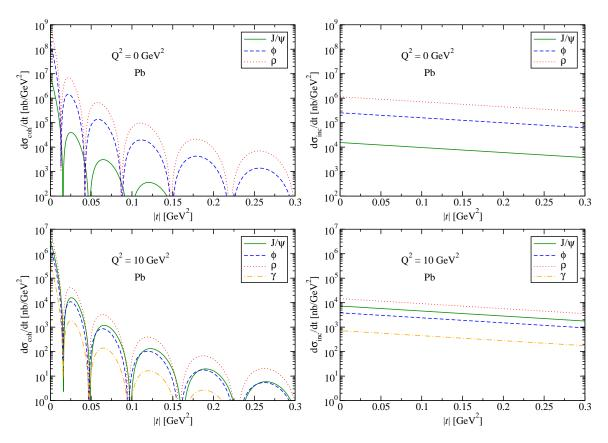


FIG. 6: (Color online) Comparison between the differential cross sections for coherent and incoherent interactions considering  $Q^2=0$  (upper panels) and  $Q^2=10~{\rm GeV}^2$  (lower panels).

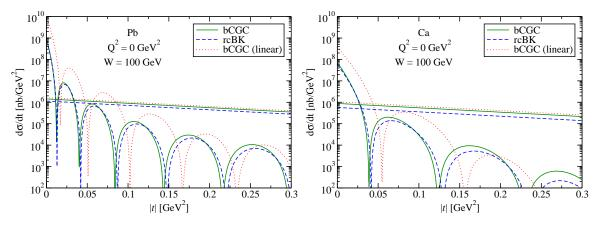


FIG. 7: (Color online) Comparison between non linear and linear predictions for the differential cross sections in coherent and incoherent interactions.

- [16] A. Caldwell and H. Kowalski, Phys. Rev. C  $\bf 81,\,025203$  (2010).
- [17] E. R. Cazaroto, F. Carvalho, V. P. Goncalves, M. S. Kugeratski and F. S. Navarra, Phys. Lett. B 696, 473 (2011)
- [18] T. Lappi and H. Mantysaari, Phys. Rev. C 83, 065202 (2011)
- [19] T. Toll and T. Ullrich, Phys. Rev. C 87, 024913 (2013)
- [20] J. T. Amaral, V. P. Goncalves and M. S. Kugeratski, Nucl. Phys. A 930, 104 (2014)
- [21] T. Lappi, H. Mantysaari and R. Venugopalan, Phys. Rev. Lett. 114, 082301 (2015)
- [22] V. P. Gonçalves and D. S. Pires, Phys. Rev. C 91, 055207 (2015)
- [23] B. Z. Kopeliovich, J. Nemchik, A. Schafer and A. V. Tarasov, Phys. Rev. C 65, 035201 (2002).

- [24] N. Armesto, Eur. Phys. J. C 26, 35 (2002).
- [25] V. N. Gribov, Sov. Phys. JETP 30, 709 (1970) [Zh. Eksp. Teor. Fiz. 57, 1306 (1969)].
- [26] H. Kowalski, L. Motyka and G. Watt, Phys. Rev. D 74, 074016 (2006); G. Watt and H. Kowalski, Phys. Rev. D 78, 014016 (2008)
- [27] H. G. Dosch, T. Gousset, G. Kulzinger and H. J. Pirner, Phys. Rev. D55, 2602 (1997).
- [28] J. Nemchik, N. N. Nikolaev, E. Predazzi and B. G. Zakharov, Z. Phys. C 75, 71 (1997)
- [29] J. R. Forshaw, R. Sandapen and G. Shaw, Phys. Rev. D 69, 094013 (2004)
- [30] H. Kowalski and D. Teaney, Phys. Rev. D 68, 114005 (2003)
- [31] J. P. B. C. de Melo and T. Frederico, Phys. Rev. C 55, 2043 (1997).
- [32] V. P. Goncalves, M. V. T. Machado and A. R. Meneses, Eur. Phys. J. C 68, 133 (2010).
- [33] V. P. Goncalves and M. V. T. Machado, Phys. Rev. C 84, 011902 (2011); V. P. Goncalves, B. D. Moreira and F. S. Navarra, Phys. Rev. C 90, no. 1, 015203 (2014); V. P. Goncalves, B. D. Moreira and F. S. Navarra, Phys. Lett. B 742, 172 (2015).
- [34] J. Jalilian-Marian, A. Kovner, L. McLerran and H. Weigert, Phys. Rev. D 55, 5414 (1997); J. Jalilian-Marian, A. Kovner and H. Weigert, Phys. Rev. D 59, 014014 (1999), ibid. 59, 014015 (1999), ibid. 59 034007 (1999); A. Kovner, J. Guilherme Milhano and H. Weigert, Phys. Rev. D 62, 114005 (2000); H. Weigert, Nucl. Phys. A703, 823 (2002); E. Iancu, A. Leonidov and L. McLerran, Nucl. Phys. A692, 583 (2001); E. Ferreiro, E. Iancu, A. Leonidov and L. McLerran, Nucl. Phys. A701, 489 (2002).
- [35] I. I. Balitsky, Phys. Rev. Lett. 81, 2024 (1998); Phys. Lett. B 518, 235 (2001); I.I. Balitsky and A.V. Belitsky, Nucl. Phys. B 629, 290 (2002).
- [36] Y.V. Kovchegov, Phys. Rev. D 60, 034008 (1999); Phys. Rev. D 61 074018 (2000).
- [37] J. L. Albacete, N. Armesto, J. G. Milhano and C. A. Salgado, Phys. Rev. D80, 034031 (2009).
- [38] A. H. Rezaeian and I. Schmidt, Phys. Rev. D 88, 074016 (2013)